DRL-Based Optimization for AoI and Energy Consumption in C-V2X Enabled IoV

Zheng Zhang, Qiong Wu, *Senior Member, IEEE*,

Pingyi Fan, *Senior Member, IEEE*, Nan Cheng, *Senior Member, IEEE*,

Wen Chen, *Senior Member, IEEE*, and Khaled B. Letaief, *Fellow, IEEE*

Abstract

To address communication latency issues, the Third Generation Partnership Project (3GPP) has defined Cellular-Vehicle to Everything (C-V2X) technology, which includes Vehicle-to-Vehicle (V2V) communication for direct vehicle-to-vehicle communication. However, this method requires vehicles to autonomously select communication resources based on the Semi-Persistent Scheduling (SPS) protocol, which may lead to collisions due to different vehicles sharing the same communication resources, thereby affecting communication effectiveness. Non-Orthogonal Multiple Access (NOMA) is considered a potential solution for handling large-scale vehicle communication, as it can enhance the Signal-to-Interference-plus-Noise Ratio (SINR) by employing Successive Interference Cancellation (SIC), thereby reducing the negative impact of communication collisions. When evaluating vehicle communication performance, traditional metrics such as reliability and transmission delay present certain contradictions.

Zheng Zhang and Qiong Wu are with the School of Internet of Things Engineering, Jiangnan University, Wuxi 214122, China (e-mail: zhengzhang@stu.jiangnan.edu.cn, qiongwu@jiangnan.edu.cn).

Pingyi Fan is with the Department of Electronic Engineering, Beijing National Research Center for Information Science and Technology, Tsinghua University, Beijing 100084, China (email: fpy@tsinghua.edu.cn).

Nan Cheng is with the State Key Lab. of ISN and School of Telecom-munications Engineering, Xidian University, Xi'an 710071, China (e-mail: dr.nan.cheng @ ieee.org)

Wen Chen is with the Department of Electronic Engineering, Shanghai JiaoTong University, Shanghai 200240, China (e-mail: wenchen@sjtu.edu.cn)

K,B. Letaief is with the Department of Electrical and Computer Engineer-ing, the Hong Kong University of Science and Technology (HKUST), HongKong (email:eekhaled@ust.hk).

Introducing the new metric Age of Information (AoI) provides a more comprehensive evaluation of communication system. Additionally, to ensure service quality, user terminals need to possess high computational capabilities, which may lead to increased energy consumption, necessitating a trade-off between communication energy consumption and effectiveness. Given the complexity and dynamics of communication systems, Deep Reinforcement Learning (DRL) serves as an intelligent learning method capable of learning optimal strategies in dynamic environments. Therefore, this paper analyzes the effects of multi-priority queues and NOMA on AoI in the C-V2X vehicular communication system and proposes an energy consumption and AoI optimization method based on DRL. Finally, through comparative simulations with baseline methods, the proposed approach demonstrates its advances in terms of energy consumption and AoI.

I. INTRODUCTION

The Internet of Vehicles (IoV) technology is the foundation for the development of autonomous driving and intelligent transportation [1]–[5]. In the future, IoV will be equipped with high-quality wireless services, including high-resolution radar perception capabilities and high-data-rate communication technologies between intelligent vehicles [6]–[11]. This will meet the diverse needs of users for vehicle applications such as automatic navigation, and collision warning, provided that timely access to the required data, videos, web pages, and other content is ensured for vehicle users through requests [12]–[16]. The traditional approach requires vehicles to first communicate with base stations, then accessing data stored in data centers through the access core backbone network, and finally, the data center returns the requested data [17]–[20]. It is evident that this method experiences long end-to-end delays and has limited bandwidth for data return [21]–[24].

C-V2X is defined by 3GPP, with "V" representing vehicles and "X" indicating communication with other vehicles, network infrastructure, road infrastructure, pedestrians, and so on [25], [26]. The issue of long end-to-end delays is addressed by V2V communication within this framework. In C-V2X mode 4, resources are autonomously selected by vehicular user equipment without reliance on cellular infrastructure, thus resolving issues of excessive delay and overhead [27]–[29]. In mode 4, the automatic selection of communication resources by vehicles is termed as SPS, which is based on a distributed sensing-based semi-persistent resource scheduling protocol [30], [31]. Semi-persistence is exemplified by vehicles being able to choose one of the standardized Resource Reservation Intervals (RRI) and then determining the corresponding

number of communication slots. However, this method may lead to collision risks as the same resources may be reserved by vehicles [32]–[34].

NOMA is a potential solution to address collision risks in C-V2X communication. It is a promising technology for handling large-scale vehicle communication [35]–[37]. NOMA can help alleviate performance degradation in terms of latency and packet reception probability caused by high vehicle density [38]. SIC is currently a detection technique can decode signals from multiple users occupying the same resource by leveraging their different signal strengths, thereby reducing interference in the SINR and minimizing latency, thus mitigating the impact of collisions [39].

In communication systems, the environment can be influenced by various factors such as changes in user numbers, fluctuations of channel conditions, and the presence of interference [40]–[43]. These factors make the optimal design of communication systems extremely complex [44], [45]. DRL algorithms can learn adaptive strategies in dynamic and complex environments [46]–[49]. Which can gradually learn the optimal strategy to achieve maximum long-term rewards, thus maximizing system performance [50], [51]. Which has been successfully applied in many fields, including but not limited to robotics, natural language processing, and vehicular communication networks [52], [53].

In existing engineering and 3GPP standards, AoI is the latest metric for measuring communication effectiveness [54], [55]. This is because lower delay or higher reliability both result in lower average AoI, indicating better timeliness of communication [56]. AoI refers to the time interval between the current time and the generation time of the data to be transmitted or received. If the average AoI at the receiving end is large, it means that the received data was generated a long time ago, indicating poor timeliness of communication. Currently, AoI is used in applications like ultra-reliable, industrial networks and low-latency communication. [57]–[59]. Therefore, low AoI facilitates the satisfaction of ultra-high data transmission rates, high-density connections, and high mobility to a great extent. However, to ensure these services, user terminals need to have high computing power for real-time signal processing, which may quickly deplete embedded batteries. Therefore, energy consumption of communication devices is also a concern [60], [61].

In summary, focusing on C-V2X vehicular networking, DRL, and performance optimization issues, considering the following factors such as the frequency of data generation from different vehicles, resource occupancy counts, resource occupancy collisions, communication energy con-

sumption, and AoI is of great theoretical significance and practical value. The main contributions are as follows[1]:

1) Consider the impact of message queuing in the C-V2X system on the AoI, along with the reconstruction of the vehicle's process of selecting resource blocks based on SPS, different arrival modes for various types of messages are modeled, and the AoI calculation model based on a multi-priority message queue involves tracking the AoI for messages with different priorities is established to analyze the role of multi-priority message queues in AoI.

2) Examinate the impacts of message transmission in the C-V2X system on AoI, where utilizing NOMA technology at the receiver end with half-duplex resource selection schemes.It will give more details on the effects of NOMA in AoI.

3) Propose a DRL scheme based on transmission power and interval in C-V2X Mode 4. Initially, vehicles reserve the resource blocks needed for the next period in the resource pool based on Mode 4 SPS selection, and obtain the number of time slots to be used according to the selected RRI. Subsequently, vehicles use broadcast communication to transmit higher priority messages to surrounding vehicles at the reserved resource's time slot. The receiver utilizes SIC-based NOMA technology to decode received messages separately. Finally, Roadside Units (RSUs) employ DRL to adjust the transmission intervals and transmit powers of each vehicle, finding the optimal strategy to optimize energy consumption and AoI in the C-V2X Mode 4 multi-type message scenario.

The rest of this paper is organized as follows. Section II reviews the related work. Section III introduces the system model and formulates the optimization problem. Section IV simplifies the formulated optimization problem and presents the near optimal solution by DRL. We carry out some simulation to demonstrate the effectiveness of our proposed method in Section V, and conclude this paper in Section VI.

II. RELATED WORK

With the increasing development of C-V2X, numerous research efforts have been initiated. In [62], a novel V2V resource allocation scheme using C-V2X technology is proposed to improve

---

[1] https://github.com/qiongwu86/DRL-Based-Optimization-for-Information-of-Age-and-Energy-Consumption-in-C-V2X-Enabled-IoV

reliability and latency in connected vehicle networks. This scheme employs a hybrid architecture where V2V links are controlled by eNodeBs, with each vehicle periodically checking the lifespan of its data packets and requesting the eNodeB to allocate the best resources link to minimize overall latency. Li et al. in [63] utilized a Markov model combined with dynamic scheduling and SPS to assess available LTE idle resources for safety services. A weighted fair queuing algorithm is proposed to schedule safety beacons using LTE reserved resources, improving safety application reliability within limited LTE bandwidth. Authors in [64] pointed out that there are four types of transmission errors in C-V2X mode 4, including half-duplex errors, resource duplication, insufficient link budget, and failures due to channel fading. The first two are caused by the unique SPS resource selection scheme at the MAC layer.

NOMA, based on power-domain multiplexing, can enhance spectrum efficiency by allowing different users to share the same resources with power multiplexing. In [65], the authors addressed the random access problem in NOMA-based backscatter communication networks with quality of service guarantees for the first time. They developed an iterative algorithm using the Dinkelbach method and quadratic transformation method to maximize user energy efficiency under constraints such as meeting QoS requirements and continuous interference elimination for SIC. [66] investigated energy efficiency maximization in NOMA-MIMO systems based on terahertz (THz) communication for the first time. They proposed a rapid convergence scheme for user clustering in THz-NOMA-MIMO systems using an enhanced K-means learning algorithm based on channel correlation characteristics. This approach maximizes the energy efficiency of cache-enabled systems even with imperfect SIC, achieving faster convergence and lower power consumption, thus realizing higher energy efficiency in terahertz cache networks. Seo et al. in [67] studied NOMA random access based on channel inversion with multi-level target powers. This ensures that the receiving power at the base station can be one of two target values to guarantee the power difference for SIC. Compared to OMA, the maximum receiving power can be increased from 0.368 to 0.7. NOMA shows potential in optimizing communication performance by improving energy efficiency.

In recent years, DRL has become commonplace for performance optimization. Ron et al. proposed a method for optimizing device transmission power to mitigate interference in [68]. They pointed out that traditional power allocation problems are often modeled as non-deterministic polynomial time hard (NP-hard) combinatorial optimization problems with linear constraints, making traditional optimization methods ineffective. Therefore, they employed DRL algorithms

to optimize vehicle transmission power and achieve D2D communication under cellular network conditions, demonstrating the potential advantages and effectiveness of DRL algorithms in optimizing power in communication. In [69], a novel approach combining resource allocation, power control, and DRL was proposed to improve D2D communication quality in critical mission communications. The DRL method based on spectrum allocation strategy enables D2D users to autonomously select channels and power, significantly improving system capacity and spectrum efficiency while minimizing interference to cellular users. Experimental results demonstrated that the method effectively improves resource allocation and power control, providing an efficient optimization solution for critical mission communications. In [70], the authors explored resource allocation problems in hybrid radio-frequency and visible light communication networks to improve network throughput and energy efficiency. Traditional methods perform poorly when faced with dynamic channels and limited resources, and heuristic methods have limited adaptability to channel and user demand changes, requiring increased communication overhead. Therefore, distributed algorithm based on DRL can adapt to network changes and optimize user transmission power to achieve target data rates, providing an effective solution for resource allocation problems in hybrid radio-frequency and visible light communication networks. This is the motivation of us doing this work.

The Information Age is used to analyze applications with timeliness requirements, mainly measure the timeliness of information in queues and transmission systems. Literature [71] analyzed the average AoI in multi-source node queuing systems considering data packet Poisson arrivals and exponential service times under Last-Come First-Served (LCFS) and First-Come First-Served (FCFS) queuing disciplines. A new, lower complexity simplification technique was proposed to evaluate the average AoI in finite-state continuous-time queuing systems. [72] considered scenarios where multiple source node-destination node pairs share the same channel and tried to minimize the average age of all source node-destination node pairs through link scheduling. It was first proven that the age minimization link scheduling problem is an NP-hard problem. Then, an optimal solution was given using integer linear programming methods, and a highly scalable steepest age descent algorithm was proposed, which has near-optimal performance and fast convergence speed.

Based on our investigation, there is no existing work in the current C-V2X vehicular networking environment that considers the role of multi-priority message queues in various aspects of message AoI, and optimizes communication performance by mitigating the impact of resource

collisions through NOMA technology in this scenario. Which motivates us to conduct this work. Furthermore, building upon this foundation, we aim to utilize receiver AoI and communication energy consumption as performance metrics for the V2V direct communication mode of C-V2X. Additionally, we will further consider the resource selection characteristics of C-V2X and employ a DRL algorithm for RRI and vehicle transmission power, while ensuring lower AoI and communication energy consumption.

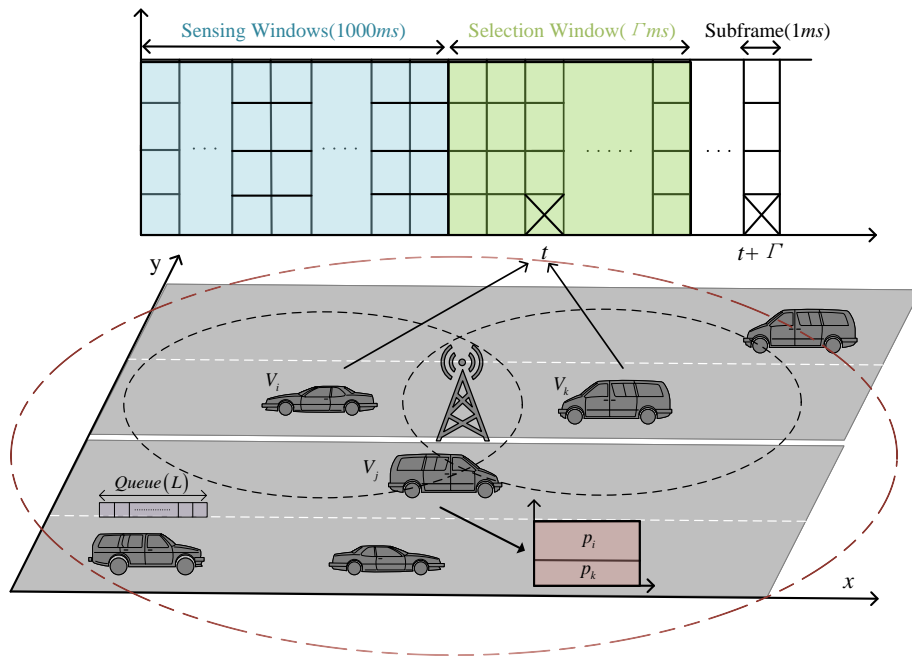## III. System Model And Problem Formulation

Fig. 1: C-V2X IoV system

A. Scenario description

Fig. 1 shows a C-V2X vehicular networking system. Assuming a highway divided into two lanes in each direction, with vehicles randomly distributed and moving at uniform speeds. Vehicles closer to the center lane travel faster, mimicking real highway scenarios. Each vehicle considers other vehicles within a circular area of radius w as potential receivers. Each vehicle maintains a message queue to store newly generated but unprocessed message data, with a maximum queue length of L, following the policy of FCFS. If the number of messages in the queue reaches L, newly generated messages are discarded due to overflow.

TABLE I: The summary for notations.

Notation	Description	Notation	Description
N_v	The total count of vehicles.	D	The length of the highway.
y_i^t	The distance between vehicle i along the y-axis and the origin at time slot t.	x_i^t	The distance between vehicle i along the x-axis and the origin at time slot t.
v	Vehicle speed.	F	Number of lanes.
f	Lane index.	d_y	The width of a lane.
w	Maximum distance at the receiver.	L	The maximum length of the message queue.
RB_i^t	The time slot where vehicle i reserves resources.	γ	Discount factor.
t_{rk}	The time slot when the vehicle is preparing to re-reserve resources.	m_i^t	The remaining amount of reserved resources that can be used.
T_w	Resource selection buffer time.	T_s	Select the time slot to reserve resources.
SPS	The method for vehicles to autonomously choose communication resources.	SW	The value of the reselection counter for vehicles.
RC	The value of the reselection counter for vehicles .	RRI	Resource selection buffer time.
Γ_i^t	The RRI size selected by vehicle i.	β_i^t	Has vehicle i transmitted messages.
α_i^t	Is there a message generated for vehicle i.	K_H	Number of repeated transmissions of HPD.
K_D	Number of repeated transmissions of DENM.	T_H	HPD repeat transmission interval.
T_D	DENM repeat transmission interval.	ρ	Whether each priority message was transmitted.
b	The position of the message in queue.	$\varphi_{i,n}^{t,b}$	AoI of messages at position b in queue n of i.
$\Phi_{i \to j}^t$	the AoI of the receiving end j for vehicle i.	u_i^t	Indicates that i transmitted the message to j.
W	Communication resource channel bandwidth.	R_{th}^t	Transmission rate threshold.
G	The size of the transmitted message.	η	SINR for communication.
p_i^t	The transmission power of vehicle i at time slot t.	h	Channel gain.
p_n^2	Noise energy.	l_i	Communication time of vehicle i.
P_{col}	Resource collision probability.	π	The probability that the vehicle is at the moment when it is ready to select resources.
CSR	The number of resources in SW.	ε_i^t	Energy consumption of vehicle i in time slot t.
E_i^t	The total energy consumption generated by vehicle i occupying a reserved resource.	$\bar{E}$	Average energy consumption.
$\bar{\Phi}$	Average AoI in receiver.	ω_1	The weighting factor of energy consumption in the reward function.
ω_2	The weight factor of AoI in the reward function.	a_i^t	The action of vehicle i in time slot t.
s_i^t	The state of vehicle i in time slot t.	N_i	Number of receivers for vehicle i.
d_i	The average distance between vehicle i and the receiver.	Rn	The ratio of receivers who successful communications to all receivers.
θ_Q	The weights of the state-action value function in strategy networks.	θ_x	The weights of the transition function strategy network.
lr_Q	Learning rate of value Q approximation function.	lr_x	Learning rate of state action transition approximation function.
τ_Q	The objective change rate of the approximate function of the value function.	τ_x	The objective change rate of the approximate function of state action transition.
M	Replay memory size.	B	Sample size.

Each vehicle in C-V2X utilizes the SPS scheme to reserve communication resources for itself. When new messages enter the message queue, vehicles check if they have any reserved communication resources. If not, they establish a Selection Window (SW) at that moment. The SW serves as a time window, indicating the duration within which the vehicle can reserve resources for itself in the future. This time window, along with its corresponding frequency domain, forms a time-frequency multiplexing structure capable of providing communication resources, known as the resource pool. Vehicles, after partitioning the resource pool, assess the occupancy of resources in the previous one thousand subframes based on metrics like Reference Signal Received Power (RSRP) and Received Signal Strength Indicator (RSSI) to determine suitable resources for communication. They then randomly reserve some of these resources for future use. Vehicles determine the RRI based on the size of the SW, i.e., the duration of the resource pool. Additionally, vehicles calculate the number of times they can use the resources according to the protocol and store it as a Reselection Counter (RC). Each time the resources are used for transmission, the RC is decremented until it reaches zero, at which point the vehicle waits for the process to repeat when a new message enters the queue. This resource selection method can lead to overlapping SW when multiple vehicles determine their SW at roughly similar times, resulting in collisions where they reserve the same resource for future broadcast communication.

When many vehicles simultaneously occupy the same resource, then the vehicles as receivers use SIC-based NOMA to decode messages in descending order of power. Lower-power messages are treated as interference and excluded after decoding the highest power message, thereby improving the SINR of each message and reducing the AoI resulting from communication failures. AoI reflects the time spent in queuing and transmission processes, where the queuing process is affected by packet generation rate or RRI, and the other process is influenced by success rate or delay. Reducing RRI decreases AoI but increases energy consumption and collision probability, affecting SINR and increasing AoI. Reducing transmission power can decrease energy consumption but also reduces SINR, leading to increased AoI. Hence, there is a need to mitigate collision effects and jointly optimize energy consumption and AoI.

An RSU with a coverage radius of R is placed at the roadside, capable of sending resource selection notifications to vehicles entering its coverage area. In each time slot, vehicles check whether resource reselection is needed and select RRI size and transmission power based on information provided by the RSU. Through trained policies, the RSU can choose appropriate

actions based on vehicle status to optimize AoI and energy consumption. Table I summarizes the symbols used in this part.

B. Vehicle motion model

Assuming all vehicles are randomly distributed across various lanes of a bidirectional highway, let (x, y) denote the position of vehicle i at time t, with the lower-left corner of the highway in Fig. 1 as the coordinate origin. Let x and y represent the distances of vehicle i along the x-axis and y-axis from the origin at time t, respectively. It is assumed that the position of each vehicle is updated with each time step

$$x_i^{t+1} = x_i^t + \delta v_i^f \tau, x_i^t \in [0, D], \tag{1}$$

where D represents the length of the highway, δ indicates the direction of vehicle travel, where $\delta = 1$ represents the x-axis direction, and $\delta = -1$ represents another direction. The speed v_i^f is defined as $v_{max} - 20 \left| f_i - F/2 + (\delta - 1)/2 \right|$ on lane f, with v_{max} representing the maximum vehicle speed. The relationship between y and the lane index f of vehicle i is as follows

$$y_i = f_i d_y - y_0, \tag{2}$$

where d_y represents the distance between two lanes in the y-axis direction on the highway, and y_0 denotes half of d_y.

C. Resource reservation model

In C-V2X Mode 4, the process of resource reservation using SPS is mainly divided into three steps: (1) When vehicles transmit a new packet and the RC is 0, it must reserve new resources within the SW. (2) The vehicle first creates a resource list, L_A, which contains resources that can be reserved. These resources include those that may be occupied by other vehicles within a certain period after the packet is generated, provided that the RSRP exceeds a threshold, or resources that have been occupied by the vehicle itself in each SW-sized time interval before the packet generation. (3) From L_A, the vehicle selects 20% of the total number of resources with the lowest RSSI to create list L_C, for random reservation by the vehicle.

Due to the periodic nature of resource occupation by vehicles using SPS, assumed to be the time slots where reserved resources are located. When the RC of the currently occupied resources becomes 0, it needs to be determined whether the queue is empty. If it is not empty, there is
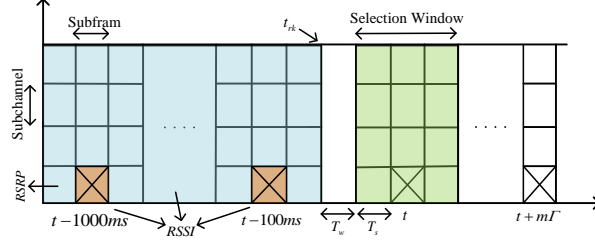
Fig. 2: Schematic diagram of communication resource reservation

a probability P_{rk} of continuing to use the currently occupied resources, and a probability of $1 - P_{rk}$ of re-selecting resources. In both cases, RC is reassigned, the time slot of the resources that the vehicle will occupy is represented as

$$RB_i^t = t_{rk} + \Gamma_i^t + m_i^t \Gamma_i^t, \tag{3}$$

$$RB_i^t = t_{rk} + T_w + T_s + \Gamma_i^t + m_i^t \Gamma_i^t, \tag{4}$$

the variables t_{rk}, Γ, m, T_w, and T_s represent the time slot for vehicles to prepare for re-reserving resources, the size of RRI, the remaining number of times the current resources can be occupied (RC does not decrease if no packets are sent during occupancy), the resource selection buffer time from 0 to 3, and the time interval from the start of the vehicle's SW to the subframe where the resource is selected, as shown in Fig. 2. And the t and $t + m\Gamma$ in Fig. 2 represent the position (space occupying) of RB_i^t. Unlike Eq.4, the situation represented by Eq.3 does not require waiting for T_w and T_s.

If the queue is determined to have no messages in queue, the vehicle needs to wait for the arrival of the first message in the queue before starting to select resource blocks, then RB is represented as

$$RB_i^t = t_a + T_w + T_s + \Gamma_t + m_i^t \Gamma_t, \tag{5}$$

where t_a is the arrival time of the first packet in the queue. When $RC \neq 0$, its expression along with m is as follows:

$$RC_i^{t+1} = RC_i^t - \beta_i^t, \tag{6}$$

$$m_i^{t+1} = m_i^t + \left\lfloor \frac{t}{RB_i^t} \right\rfloor \left\lceil \frac{RC_i^t}{RC_i^0} \right\rceil, \tag{7}$$

where β is a binary variable indicating whether the vehicle transmits messages from the queue, and RC_i^0 is the initial value of RC.

D. Message queue model

The status of the message queue depends on message generation and processing. Assuming the queue has a capacity of L, the length of the queue, q, can be be updated as follows

$$q_i^{t+1} = \begin{cases} q_i^t & \alpha_i^t = 0, \beta_i^t = 0 \\ q_i^t - 1 & \alpha_i^t = 0, \beta_i^t = 1 \\ q_i^t + 1 & \alpha_i^t = 1, \beta_i^t = 0 \\ q_i^t & \alpha_i^t = 1, \beta_i^t = 1 \\ L & q_i^t = L, \beta_i^t = 0 \end{cases}, \tag{8}$$

where α_i^t represents whether vehicle i generates a message at time slot t. This queue applies to all message types in C-V2X.

C-V2X mode 4 includes four types of messages: High-Priority Data (HPD), Decentralized Environmental Notification Messages (DENM), Cooperative Awareness Messages (CAM), and Miscellaneous High-Density Data (MHD). Their priority order is HPD > DENM > CAM > MHD. CAM-type packets are generated periodically with a period of $\frac{1}{T_c}$, while other types of packets are generated trigger-based. Therefore, the expression for whether CAM messages are generated is

$$\alpha_{i,c}^t = 1 - \left\lceil \frac{t \bmod T_c}{T_c} \right\rceil, \tag{9}$$

when t is an integer multiple of T_c, $a_i^t = 1$, indicating the occurrence of a new CAM message. The probability of new packet generation for other types follows the probability mass function of the Poisson distribution

$$P(arr_{i,n}^t = 1) = \lambda_n e^{-\lambda_n}, \tag{10}$$

where $arr_{i,n}^t = 1$ indicates that a new package has been generated, λ_n is the arrival rate, n encompasses the production quantities of the three message types mentioned above within a certain time period. To ensure the successful transmission of new messages generated by HDM and DENM, each needs to be retransmitted K_H and K_D times respectively, with this retransmission process occurring periodically at intervals of T_H and T_D. At this point, the queue arrival rate is the sum of the production rates of the four message types, while the processing rate is the reciprocal of the RRI, $\frac{1}{\Gamma}$.

In a single priority queue, β_i^t is equivalent to ρ_i^t, representing the successful transmission of different message types in the single priority queue. This occurs when there are messages queued

in the vehicle queue and reserved communication resources are available for use at that moment. The expression is as follows

$$\rho_i^t = \left\lfloor \frac{t}{RB_i^t} \right\rfloor \left\lceil \frac{q_i^t}{L} \right\rceil. \tag{11}$$

The expression indicates that the transmission operation can only be completed when the estimated time equals the current time and the queue is not empty.

When operating under a single priority scheme, multiple message types share the total message generation rate and processing rate. However, in a multi-priority scheme, each message type has its own message generation rate, and the processing rate for high-priority messages equals the total processing rate of the single-priority queue. Therefore, in a multi-priority queue, the ratio of the message generation rate to the processing rate for high-priority messages is relatively low, ensuring a lower AoI for high-priority messages.

Therefore, four corresponding FIFO queues are established for different types of signals, all with a capacity of L and a queue length of q. New messages of the corresponding type can only be added to the queue when the queue satisfies $q < L$, and transmission opportunities leaving the queue need to prioritize high-priority messages. Transmission opportunity refers to the vehicle being able to use reserved resources in a particular time slot t. Therefore, the expressions for the transmission action β and the determination of whether each queue can be transmitted ρ in the multi-priority queue are as follows

$$\begin{cases} \beta_{i,H}^t = 1, \beta_{i,C}^t = 0 & \rho_{i,H}^t = 1 \\ \beta_{i,H}^t = 0, \beta_{i,C}^t = 1 & \rho_{i,C}^t(1 - \rho_{i,H}^t) = 1 \\ \beta_{i,H}^t = \beta_{i,C}^t = 0 & otherwise \end{cases}, \tag{12}$$

$$\rho_{i,n}^t = \left\lfloor \frac{t}{RB_i^t} \right\rfloor \left\lceil \frac{q_{i,n}^t}{L} \right\rceil, \tag{13}$$

the n in $\rho_{i,n}^t$ includes four types of messages, such as $\rho_{i,H}^t$ and $\rho_{i,C}^t$. Because it is determined in order of priority, the expression involving two priority queues can reflect the relationship between different queue β values.

E. AoI model

The changes in AoI are shown in Fig. 3. The solid line represents the AoI of receiver , the dark dashed line represents the AoI of the messages in the queue, both of which increase over time. The light dashed line represents the time slot that the vehicle can occupy for resource
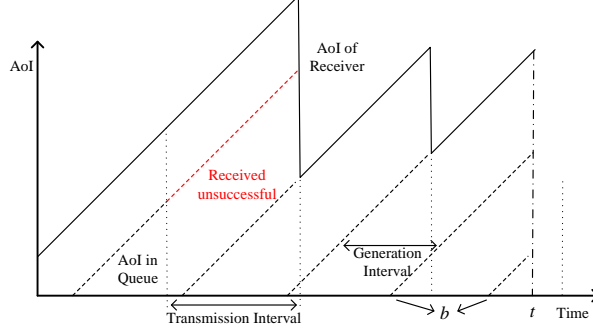
Fig. 3: Changes in AoI.

transmission. If the transmission is successful, the AoI of receiver will be updated to the AoI of received message. The red dashed line indicates that the message transmission has failed, and the receiver is unable to update the AoI, so it will continue to grow on the previous basis. In addition, b represents the position of each message in the queue.

The AoI increases with each subframe while messages are queued, but it stops increasing when they leave the queue. Therefore, the AoI expression for four types of packets in corresponding queue is

$$\varphi_{i,n}^{t+1,b} = \begin{cases} \varphi_{i,n}^{t,b+1} + 1 & \beta_{i,n}^t = 1 \\ \varphi_{i,n}^{t,b} + 1 & \beta_{i,n}^t = 0 \end{cases}, \tag{14}$$

where n encompasses four queues, $\phi_{i,n}^{t,b}$ represents the AoI of the message at position b in queue n of vehicle i at time slot t. When β=1, the positions of all packets in the queue, except for the head, will shift. The probability of β=1 is the processing rate, since the processing rate in C-V2X is expressed as $\frac{1}{\Gamma}$, and the RRI will affect AoI of the message in queue.

The accumulated AoI in communication process represents the time elapsed between two consecutive transmissions from the transmitter to the receiver. Moreover, since received messages reflect the transmitter's conditions at transmission time, the receiver must retain their AoI to show the freshness of the data about the transmitter. The expression for the AoI of vehicle j as receiver with respect to vehicle i as transmitter

$$\Phi_{i\to j}^{t+1} = \begin{cases} \varphi_{in}^{t.1} + l_{i\to j}^t & u_{i\to j}^t = 1 \\ \Phi_{i\to j}^t + 1 & u_{i\to j}^t = 0 \end{cases}, \tag{15}$$

where $\Phi_{i\to j}^t$ represents the AoI of vehicle j with respect to vehicle i at time t, l denotes the transmission delay, and u represents the transmission situation. When $u = 1$, it indicates that vehicle i successfully transmits the message to j. In this case, the AoI at vehicle j is calculated by adding the transmission time to the AoI of the packet at the head of the highest priority

queue broadcasted by vehicle i. When $u = 0$, it signifies a transmission failure, and thus $\Phi_{i \to j}^t$ is updated to $\Phi_{i \to j}^{t-1}$ plus one time slot. Due to the unique way of allocating resources for vehicles in C-V2X mode 4, each transmission failure necessitates waiting for a time interval equal to the RRI size, resulting in an increase in $\Phi_{i \to j}^t$ by Γ.

F. Communication model

The size of the resources in mode 4 is variable, and the vehicle occupies the required bandwidth W based on the message size G, while the expression for the transmission rate threshold is

$$R_{th}^t = W_i \log_2(1 + \eta_{th}), \tag{16}$$

Among them $R_{\text{th}} = G$, because the time for the data packet to complete data transmission should not exceed one slot, that is, $\frac{G}{R} \leq 1$. Then calculate the SINR threshold based on the bit width and R_{th}^t as follows

$$\eta_{th} = 2^{R_{th}^t/B_i} - 1 = 2^{G_i/B_i} - 1, \tag{17}$$

Different distances between vehicles at different times cause varying channel damage in communication, resulting in the receiving end receiving at different communication rates on different channels. And vehicles can use different resources at the same time, so the vehicle as receiver gets message at varying rates across these resources. When the vehicle only receives one message at most within a resource, at time slot t the SINR is

$$\eta_{i \to r}^{t,n} = \frac{p_i^t |h_{i \to j}^{t,n}|^2}{p_n^2}, \tag{18}$$

p_i^t is the transmission power of vehicle i, $|h_{i \to j}^{t,n}|^2$ is the channel gain for communication, p_n is the noise energy, and n is the communication resource.

However, vehicles in the C-V2X model 4 system may reserve the same resource, and the collisions may occur. According to [73], the collision probability in the system can be expressed as

$$P_{col} \approx 1 - \left[1 - \left[1 - \prod_{i=0}^{\Gamma-1} \left(1 - \frac{\pi}{1-\pi i} \right) \right] \frac{1-P_{rk}}{CSR-N_v+1} \right]^{N_v-1}, \tag{19}$$

π is the probability that the vehicle is at the moment of preparing to select resources, that is, the probability that all three conditions of the vehicle queue being non empty, RC being 0, and rebooking new resources are met simultaneously. Γ is equivalent to the number of sub frames in SW, CSR represents the total number of resources in SW, which is the product of Γ and the

number of sub-channels. Therefore, CSR is proportional to Γ, and N_v is the total number of vehicles.

So when Γ remains constant, P_{col} increases with N_v. The expression for the SINR of the receiver when a collision occurs is

$$\eta_{i \to j}^{t,n} = \frac{p_i^t \left| h_{i \to j}^{t,n} \right|^2}{\sum\limits_{g \in N_g} p_g^t \left| h_{g \to j}^{t,n} \right|^2 + p_n^2}, \tag{20}$$

g represents interfering vehicles, and p_g^t is their transmitted energy. When the same resource is shared by multiple vehicles, the $\eta_{i \to j}^{t,n}$ drops, which can cause transmission failures if it's too low. Therefore, introducing SIC based NOMA to address this situation. The receiver sorts the received multiple signals according to the received power, and use the signal with the strongest received power as the target and treat other signals as interference, then decode and remove them. Then loop through the operation until the SINR of all signals is calculated. If $N_k = \left\{ k \in N \setminus i | p_{i \to j}^t \left| h_{i \to j}^{t,n} \right|^2 > p_{k \to j}^t \left| h_{k \to j}^{t,n} \right|^2 \right\}$ is a vehicle group with weaker receiving power than vehicle i, then the SINR at vehicle j for vehicle i is

$$\eta_{i \to j}^{t,n} = \frac{p_i^t \left| h_{i \to j}^{t,n} \right|^2}{\sum\limits_{k \in N_k} p_k^t \left| h_{k \to j}^{t,n} \right|^2 + p_n^2}, \tag{21}$$

It can be seen that when collisions occur, messages are transmitted over the same frequency band but with different power levels. By using NOMA to sequentially decode higher power messages first, the receiver can effectively cancel out the stronger messages before decoding the weaker ones. This process mitigates interference from stronger messages allowing the weaker signals to be decoded more accurately. Thereby increasing SINR and reducing the possibility of transmission failure caused by SINR below the threshold. And the transmission time between vehicle i and j is

$$l_{i \to j}^t = \frac{G}{W_i \log_2(1 + \eta_{i \to j}^t)}. \tag{22}$$

G. Energy consumption model

In C-V2X, the vehicle will communicate throughout the entire time slot of the reserved resources, so the energy consumption generated by the vehicle during each transmission is

$$\varepsilon_i^t = p_i^t \beta_i^t. \tag{23}$$

However, the vehicle will repeatedly occupy RC_i^0 times after each reserved resource. So E_i^t, the total energy consumption of the vehicle during this time period, is represented as

$$E_i^t = \varepsilon_i^t RC_i^0. \tag{24}$$

H. Problem formulation

Establish a joint optimization problem with the objective of minimizing the weighted average of AoI and energy consumption for all vehicles. Because the transmission interval and power determine the magnitude of AoI and energy consumption, they are used as variables for the optimization problem. Therefore, the optimization objective is

$$\min_{\Gamma^t, p^t} \left[\omega_1 \overline{E} + \omega_2 \overline{\Phi} \right] \tag{25}$$

$$s.t. \qquad p^t \in [0, P_{max}], \forall t \in \mathcal{T}, \tag{25a}$$

$$\Gamma^t \in \{20, 50, 100\}, \forall t \in \mathcal{T}, \tag{25b}$$

among them, ω_1 and ω_2 are non negative weight factors, and $\mathcal{T} = \{1, \ldots, t, \ldots, T\}$ is the set notation of time slots. Where $\overline{E}$ and $\overline{\Phi}$ represent the average energy consumption and the average AoI at the receiving end, respectively, and their expressions are:

$$\bar{E} = \frac{1}{T} \frac{1}{N_v} \sum_{t \in \mathcal{T}} \sum_{i \in N_v} E_i^t. \tag{26}$$

$$\bar{\Phi} = \frac{1}{T} \frac{1}{N_v} \frac{1}{N_v - 1} \sum_{t \in \mathcal{T}} \sum_{i \in N_v} \sum_{j \in N_v} \Phi_{i \to j}^t. \tag{27}$$

IV. DRL METHOD FOR OPTIMIZATION OF RRI AND POWER ALLOCATION

Considering the uncertain channel conditions of the C-V2X system, this section introduces an Multi-Pass deep Q-Networks (MPDQN) method based on DRL to solve the Γ and p allocation problems of vehicles in the system. Using the DRL framework to model the problem, which mainly includes states, actions, policies, and rewards. Specifically, the RSU takes action a^t based on the current state s^t and the policy, and obtains the corresponding reward r^t and the state s^{t+1} for the next time slot.

A. DRL framework

- **State:** In time slot t, vehicle i uses broadcasting to communicate with other vehicles. The number of receivers for vehicle i is N^t, and the average distance between them and vehicle i is d_i. When vehicle i transmits messages in time slot t, the ratio of the number of successful recipients to the total number is Rn, reflecting the impact of current transmission power on the communication process under uncertain channel conditions. RC^0 affects the queue message processing rate and communication frequency. Therefore, the state of vehicle i in the time slot is defined as

$$s_i^t = [N_i^t, d_i^t, Rn_i^t, RC_i^0]. \tag{28}$$

- **Action:** RSU allocates transmission intervals and power to vehicles based on their status, therefore the actions of vehicle i in time slots are defined as

$$a_i^t = [\Gamma_i^t, p_i^t]. \tag{29}$$

The Γ is a discrete value and p is a continuous value, so the MPDQN algorithm that can simultaneously make choices for actions in this situation is used to solve it. First, match each discrete action with a continuous action as part of the state, treating the two actions as one action tuple, and then select the action tuple based on the state. Therefore, in MPDQN, the action tuple of a vehicle is defined as

$$a_i^t = (\Gamma_i^t, p_\Gamma). \tag{30}$$

- **Reward function:** In this chapter, the goal of RSU is to optimize communication performance in the system, including AoI and energy consumption. Every time a vehicle selects an action, it will use it until the next reserved resource is selected. Therefore, the energy consumption generated by vehicle i during that time period and the AoI of its receiver will be weighted and averaged as the reward function. So the reward function for vehicles in time slot t is defined as

$$r_i^t = -[\omega_1 E_i^t + \omega_2 \overline{\Phi_i^t}], \tag{31}$$

$\overline{\Phi_i^t}$ is the average AoI received by vehicle i at the receiving end during this time period, expressed as

$$\overline{\Phi_i^t} = \frac{1}{T}\frac{1}{N_v}\sum_{t=1}^{T}\sum_{j\in N_v}\Phi_{i\to j}^t. \tag{32}$$

B. *Optimizing allocation based on MPDQN*

As described in [74], the optimization objective is achieved by adjusting the values of discrete action Γ and continuous action p. This means that the action space is not solely discrete or continuous, which makes traditional DRL methods inadequate. Therefore, MPDQN is needed to directly handle this situation. The agent using MPDQN first evaluates the value of each discrete action and corresponding continuous action based on the state and θ_x. It then pairs each discrete action with the continuous action that has the highest corresponding value, forming an action tuple. Finally, it identifies the action tuple with the highest value based on the state and θ_Q, determining the optimal discrete and continuous actions for the current state.

According to [75], [76], for a set of action (Γ_i^t, p_Γ), its state action value function can be expressed as $Q(s^t, a^t) = Q\left(s^t, (\Gamma, p_\Gamma)\right)$. To correspond Γ and p, define a policy network as the transition function between discrete and continuous actions in state s^t

$$p_\Gamma^t = x^Q\left(s^t, \Gamma^t; \theta_x\right), \tag{33}$$

where θ_x is the weight of the network.

Therefore, the action value function of vehicle i in state s_i^t and action (Γ_i^t, p_Γ) is

$$Q\left(s_i^t, \left(\Gamma_i^t, p_\Gamma\right)\right) = Q\left(s_i^t, \left(\Gamma_i^t, x^Q\left(s_i^t, \Gamma; \theta_x\right)\right)\right). \tag{34}$$

Using a deep neural network with network weight θ_Q to approximate $Q(s, (\Gamma), p)$, the Eq. 34 can be written as

$$Q(s_i^t, a_i^t) = Q\left(s_i^t, \left(\Gamma_i^t, x^Q\left(s_i^t, \Gamma; \theta_x\right)\right); \theta_Q\right). \tag{35}$$

Then, by updating the network weights, the optimization objective of the problem is approached, and the target value of the vehicles in the scene is defined as

$$y^t = r^t + \gamma \max_\Gamma Q\left(s^{t+1}, \Gamma^{t+1}, x^Q\left(s^{t+1}; \theta_x\right); \theta_Q\right). \tag{36}$$

The loss function of each network is defined as

$$L_Q\left(\theta_Q\right) = \mathop{\mathbb{E}}_{(s^t, (\Gamma, p_\Gamma), r^t, s^{t+1}) \sim M} \left[\tfrac{1}{2}\left(y^t - Q\left(s^t, (\Gamma, p_\Gamma); \theta_Q\right)\right)^2\right], \tag{37}$$

$$L_x\left(\theta_x\right) = \mathop{\mathbb{E}}_{s^t \sim M} \left[-\sum_{\Gamma = \{20, 50, 10\}} Q\left(s^t, \Gamma, x^Q\left(s, \Gamma; \theta_x\right); \theta_Q\right)\right]. \tag{38}$$

Finally, update the parameters through the following methods

$$\theta_Q^{t+1} = \theta_Q^t - lr_Q \nabla_{\theta_Q} L_Q\left(\theta_Q\right), \tag{39}$$

$$\theta_x^{t+1} = \theta_x^t - lr_x \nabla_{\theta_x} L_x(\theta_x), \tag{40}$$

the lr_x and lr_Q are the learning rates of the two policy networks.

Next, we will explain the algorithm in detail, with the pseudocode in Algorithm 1. Firstly, randomly initialize θ_x and θ_Q, and establish an experience replay buffer M. Next, the algorithm loops through EP segments, resetting the system model simulation parameters at the beginning of each segment. The intelligent agent outputs the action tuple (Γ_i^t, p_Γ) based on the initial network parameters, and then observes the state $s_i^1 = [N_i^1, d_i^1, Rn_i^1, RC_i^0]$ after the action is used. Then, the algorithm cycles from time slot 1 to time slot T. For each time slot t, it randomly selects with a certain probability or calculates the corresponding p for each Γ according to formula Eq. 33. Then, according to Eq. 35, the action tuple (Γ_i^t, p_Γ) with the highest Q value is obtained, and exploration noise is added. Finally, the intelligent agent will store the observed reward r, state s^{t+1}, and previous state actions as tuples $[s^t, (\Gamma^t, p^t), r^t, s^{t+1}]$ in M. When the number of tuples exceeds the size of the sample B, B tuples are taken from it to update the network parameters.

V. SIMULATION RESULTS AND ANALYSIS

A. Parameter Settings

In this section, we conducted extensive simulation experiments on the scene in Fig. 1, using Python 3.6 and MATLAB 2023b as simulation tools. Simulation was added and modified based on [77]. Assuming the length of the highway D is $500m$, the number of vehicles N_v is $20 - 50$, and the communication distance w of the vehicles is $150m$. According to the C-V2X standard, the bandwidth is set as 10 MHz and QPSK modulation for propagation. The T_C of CAM takes $100ms$, and the other three types of messages are λ set to 0.0001. The T_H, T_D, K_H and K_D are set to $100ms$, $500ms$, 8 and 5 respectively. In the simulation, the learning rates of the two networks are $lr_x = 10^{-4}$ and $lr_Q = 5 * 10^{-4}$, respectively, and the update parameters τ_x and τ_Q of the networks are both 0.01. Used replay memory size of 2000, sample size $B = 128$, discount factor $\gamma = 0.99$. In the process of selecting actions, greedy action strategies and exploration of action parameters with additive Ornstein Uhlenbeck noise are used [59]. The parameters used in the simulation are shown in Table II.

B. simulation Result

The existing work adopts genetic algorithms and random strategies as baseline algorithms for resource allocation. Therefore, we chose these two algorithms for comparison. The introduction

---
Algorithm 1: Optimization algorithm based on MPDQN

Input: γ, τ_Q, τ_x, θ_Q, θ_x

Output: optimized θ_Q, θ_x

1 Randomly initialize the θ_Q, θ_x;

2 Initialize replay experience buffer M;

3 for *episode from* 1 *to* EP **do**

4   Reset simulation parameters for the system model;

5   Receive initial observation state s_0;

6   **for** *slot* t *from* 1 *to* T **do**

7   Generate action tuples;

8   Execute action (Γ_i^t, p_Γ), observe reward r^t and new state s^{t+1} from the system model;

9   Store transition tuple $[s^t, (\Gamma^t, p_\Gamma), r^t, s^{t+1}]$;

10   **if** *number of tuples in* M *is larger than* B **then**

11   Randomly sample a mini-batch of B transitions tuples from M;

12   Update the critic network by minimizing the loss function according to Eq. (37) and Eq. (38);

13   Update the actor network according to Eq. (39) and Eq. (40).

TABLE II: Values of the parameters in the experiments.

Parameter	Value	Parameter	Value
N_v	$20 \sim 50$	L	10
D	$500m$	w	$150m$
T_C	$100ms$	λ	0.0001
K_H	8	K_D	5
Lr_Q	$5 * 10^{-4}$	lr_x	10^{-4}
P_{max}	$23dBm$	v_{min}	$60km/h$
B	128	v_{max}	$80km/h$
τ_Q	0.01	τ_x	0.01
M	2000	γ	0.99

of random strategy and genetic algorithm here is as follows

- Random policy: In C-V2X, vehicles randomly allocate power for each vehicle within the range $[0, P_{max}]$ based on the utilization of multiple priority queues and NOMA. Additionally, each vehicle's RRI is randomly assigned from the set $20, 50, 100$.

- GA-based policy: In each time slot, the RSU randomly generates a population vector based on the range of RRI and power values, as well as the population size, and uses the reward function as the fitness function. Each individual in the population represents the RRI and power allocation for all vehicle. The RSU employs a competition method to select the better individuals from the population vector based on the fitness of all individuals for crossover, generating offspring. These offspring undergo mutation operations and are then provided to the vehicles to obtain new fitness. Through multiple iterations of evolution, the crossover and mutation operations explore better actions, approaching the optimal RRI and power allocation.

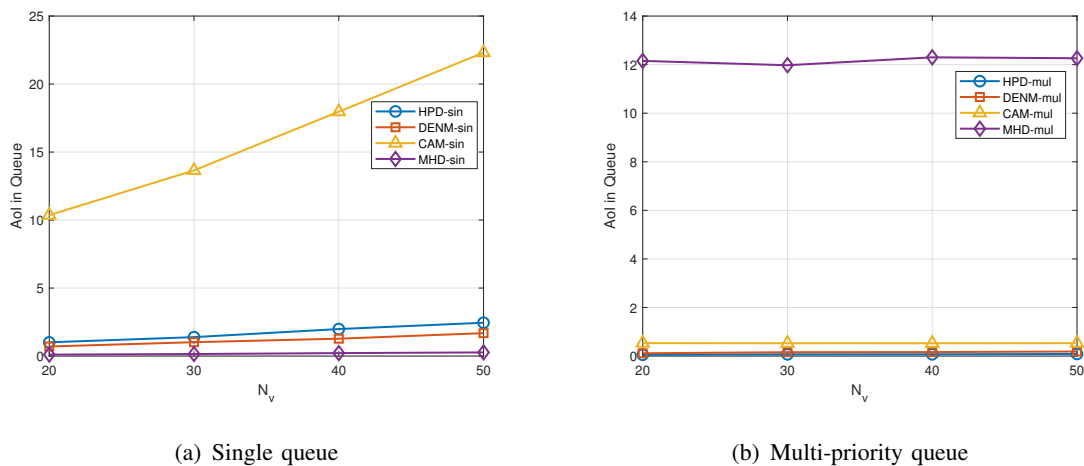(a) Single queue   (b) Multi-priority queue

Fig. 4: The AoI in queue with low processing rates.

Fig. 4(a) compares the average AoI variation for different types of messages from single-priority queue vehicles in the scenario when the Γ is selected as $100ms$. It is evident that as the number of vehicles increases, the average AoI of each message type in the queue gradually increases. Moreover, since the processing rate of vehicle message queues is $10/s$ when the $\Gamma = 100ms$, and the sum of production rates for all message types is significantly higher than this value, all message types struggle to be transmitted in a timely manner. Therefore, the relative sizes of AoI among these messages are correlated with their respective production rates. Messages with higher production rates exhibit larger AoI values. Consequently, the average AoI

of the CAM type, which has the highest production rate, is the largest. While the average AoI of the MHD message type, which has the least frequent production rate, is the smallest.

Fig. 4(b) compares the average AoI variations of messages of various types for multi-priority queue vehicles in the scenario when the RRI is 100ms. It can be observed that the higher the priority of a message, the smaller its average AoI, while the lower the priority, the larger the average AoI, ensuring the freshness of critical information when not all information transmission can be guaranteed in the communication environment. Moreover, compared to various types of messages in a single-priority queue, the average AoI of messages with higher priority becomes smaller. This is because in the presence of priorities, messages with lower priority always need to wait for messages with higher priority to be transmitted first, resulting in a lower processing rate for the queue of lower-priority messages compared to the queue of higher-priority messages. Among them, CAM-type messages show the largest variation because they have the highest message generation frequency, making them more prone to accumulation, especially when all types of messages are in a single queue. Therefore, when the priority of CAM-type messages is higher than that of MHD-type messages, the freshness of lower-priority MHD messages is sacrificed to ensure the transmission of CAM-type messages, thus reducing the average AoI.
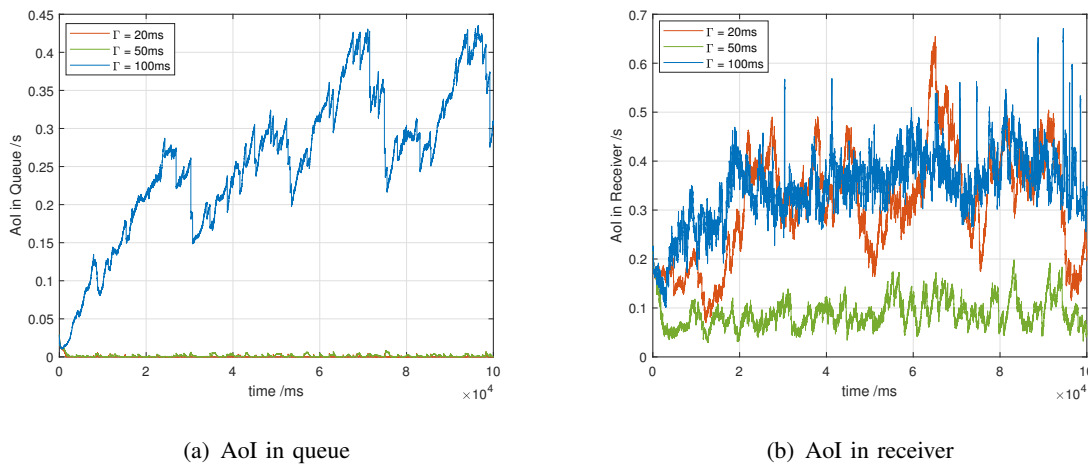

(a) AoI in queue   (b) AoI in receiver

Fig. 5: The changes of average AoI with different Γ.

When Γ is relatively small, the queue has a higher processing rate, resulting in smaller AoI for messages in the local queue. As shown in Fig. 5(a), with 30 vehicles in the scenario. Setting Γ to 20 or $50ms$ satisfies the transmission requirements of all queues, preventing message accumulation in vehicle queues and avoiding an increase in average AoI. However, when vehicles choose Γ of $100ms$, it fails to meet the transmission demands of queue messages, especially

occasional high-priority messages that further strain the processing rate, leading to an increase in AoI. Nevertheless, as depicted in Fig. 5(b), significant fluctuations occur in the AoI of receiver when the Γ is at its minimum, while vehicles selecting anΓ of $50ms$ consistently exhibit the lowest receiver AoI, significantly outperforming other selections. This indicates that vehicles choosing an Γ of $20ms$ are subjected to greater impact during transmission.

Fig. 6(a) illustrates the influence of different RRI chosen by vehicles on the average AoI at the receiver for varying numbers of vehicles. It can be observed that the AoI is consistently higher when the Γ is $100ms$, attributed to inadequate processing rates leading to excessively large queue AoI, coupled with longer communication intervals between the receiver and transmitter. Across all vehicle counts, the AoI of receiver is minimized when the Γ is $50ms$, while in scenarios with fewer vehicles, the AoI with an Γ of $20ms$ is smaller, but surpasses that of $100ms$ as vehicle count increases. Furthermore, regardless of the chosen Γ, the AoI of receiver increases as the vehicle count rises. This is due to an increase in collision probability during communication, as per Eq. (19). When the Γ is $20ms$, the likelihood of contending for the same resources as other vehicles increases, leading to more instances of resource contention and thus higher chances of collisions. As the number of vehicles in the scenario increases, the required number of reserved resources also rises, increasing the likelihood of simultaneous resource selection and consequently elevating the possibility of different vehicles reserving the same resources.
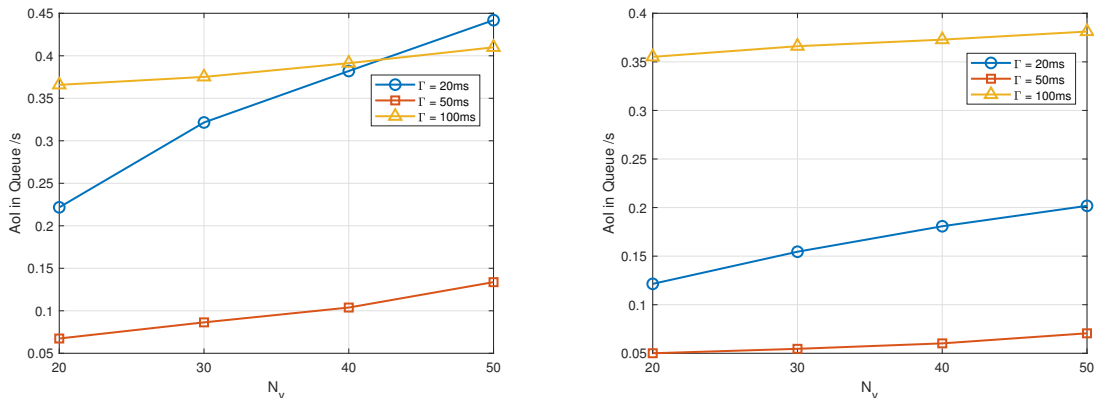

(a) C-V2X without NOMA   (b) C-V2X with NOMA

Fig. 6: The average AoI at receivers in C-V2X.

Fig. 6(b) illustrates the impact of vehicle selection of different RRI values on the average AoI at the receiver when using NOMA. Comparing with Fig. 6(a), it can be observed that NOMA improves the receiver AoI for all scenarios, particularly with the $20ms$ Γ, where the

improvement is most pronounced, reducing by approximately half. Moreover, as the N_v increases, the improvement in each scenario becomes more significant, especially in situations with higher collision probabilities. Overall, NOMA can mitigate the effects of resource collisions resulting from the half-duplex selection of communication resources in C-V2X vehicular networking systems, thus optimizing the AoI of receiver.
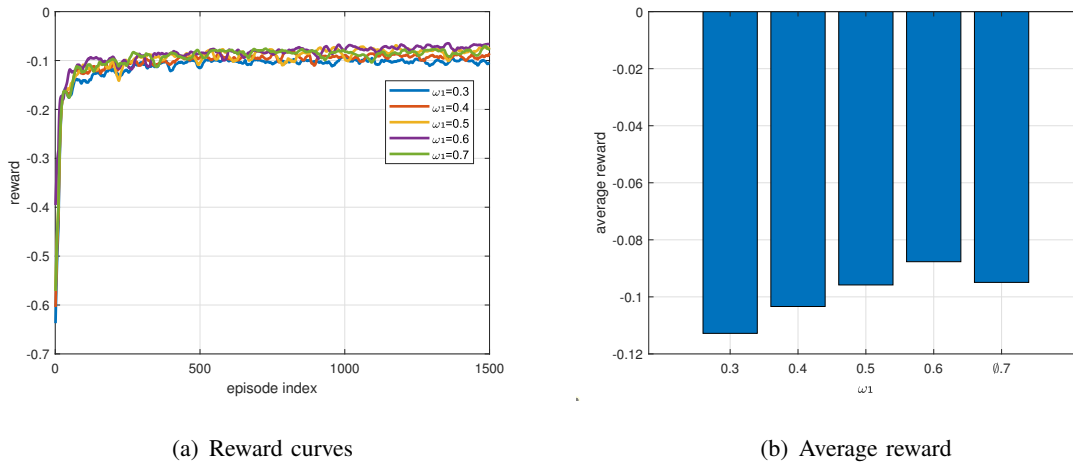
(a) Reward curves   (b) Average reward

Fig. 7: The simulation results for different values of $\omega 1$.

Fig. 7(a) illustrates the training process curves for different values of weights, ranging from 0.3 to 0.7. Values of 0.1 and 0.2 were excluded to prevent bias towards specific performance during learning. Each curve in the figure represents the average reward of all vehicles within a time slot in each segment. It can be observed that all curves fluctuate and rise moderately from 0 to 500 segments, as the agent searches for optimal RRI and power allocation parameters for the AoI of system and energy consumption. Subsequently, the curves fluctuate within a certain range, with significantly higher average rewards compared to the untrained state, indicating that the learned strategies of the agent are approaching optimality. However, the convergence fluctuation ranges vary for each curve when different network weight values are selected, especially evident in the significant difference between the best-performing curve at 0.6 and the worst-performing one at 0.3.

To better compare the impact of different values of ω_1 on rewards, the rewards of all vehicles across all segments were averaged, as shown in Fig. 7(b). It can be observed that, consistent with Fig. 7(a), although the average rewards are relatively high for different values of ω_1, the highest average reward is achieved when $\omega_1 = 0.6$ compared to other scenarios. The largest difference is observed compared to $\omega_1 = 0.3$, nearing 0.02. Therefore, selecting 0.6 as the weight size for learning strategies in other scenarios seems justified.
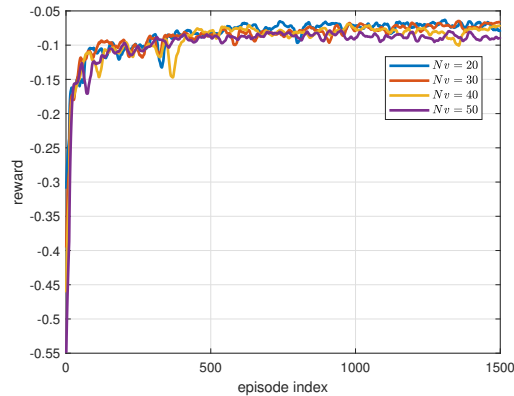
Fig. 8: Reward curves for different N_v.

Fig. 8 displays how average rewards change with different N_v. Each curve in the figure represents the average reward of vehicles within each segment. It can be observed that all curves fluctuate upwards before segment 500 and stabilize within a certain range thereafter. By examining the fluctuation range of curves for different numbers of vehicles, it is evident that with fewer vehicles, the average reward fluctuates within a higher range. And the average reward gradually decreases as the N_v increases. This is because the vehicle interference also rises, leading to an increase in AoI. To reduce the impact of increased AoI on rewards, the agent appropriately selects smaller to increase the transmission frequency of vehicles, thereby reducing the AoI of receiver. However, smaller Γ imply more transmissions, which may increase energy consumption and hence lower rewards.
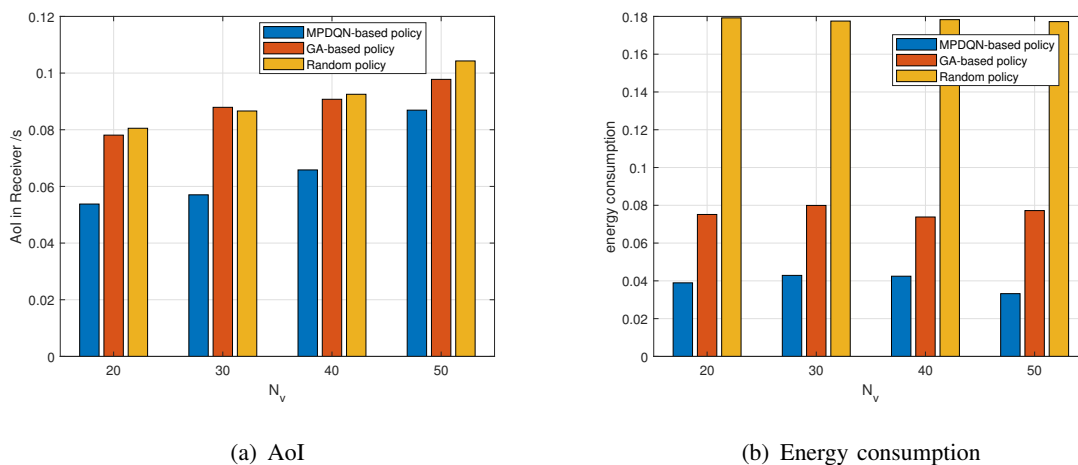

(a) AoI

(b) Energy consumption

Fig. 9: The simulation results of each scheme for different numbers of vehicles.

Fig. 9(a) compares the average sum AoI under MPDQN, GA, and random algorithms. It can be observed that under all three strategies, the average sum AoI within the system tends to

increase as the N_v increases. This is because the average AoI encompasses the AoI of all vehicles in the system acting as receivers, so as the N_v increases, both the queuing time for messages and the transmission process affect more receivers. Particularly, interference generated during transmission increases with the N_v, leading to an increase in the average AoI. Additionally, it can be seen that both MPDQN and GA algorithms generally achieve lower average AoI compared to the random strategy, with MPDQN achieving the lowest average AoI. This is because MPDQN can adaptively adjust the RRI and power based on the current state of the vehicles.

Fig. 9(b) compares the average energy consumption within the system under MPDQN, GA algorithm, and random algorithm for different N_v. It can be seen that the energy consumption fluctuates slightly with an increase in the N_v under MPDQN and GA algorithms, while the average energy consumption remains relatively stable with an increase in the seen under the random algorithm. This is because the average energy consumption is the mean of the energy consumption of all vehicles in the scenario. When using the random algorithm, the RRI and power of all vehicles in the scenario are randomly chosen, and an increase in the N_v does not significantly affect the mean energy consumption of all vehicles. However, for MPDQN and GA algorithms, both AoI and energy consumption need to be considered simultaneously. As mentioned in Fig. 9(b), when the N_v increases, the average AoI increases. However, since the weight of energy consumption is set larger than the weight of AoI, MPDQN and GA algorithms prioritize selecting relatively lower energy consumption while ensuring that the AoI remains within an acceptable range. Therefore, despite the increase in the number of vehicles, the variation in energy consumption is not as significant as the variation in AoI.

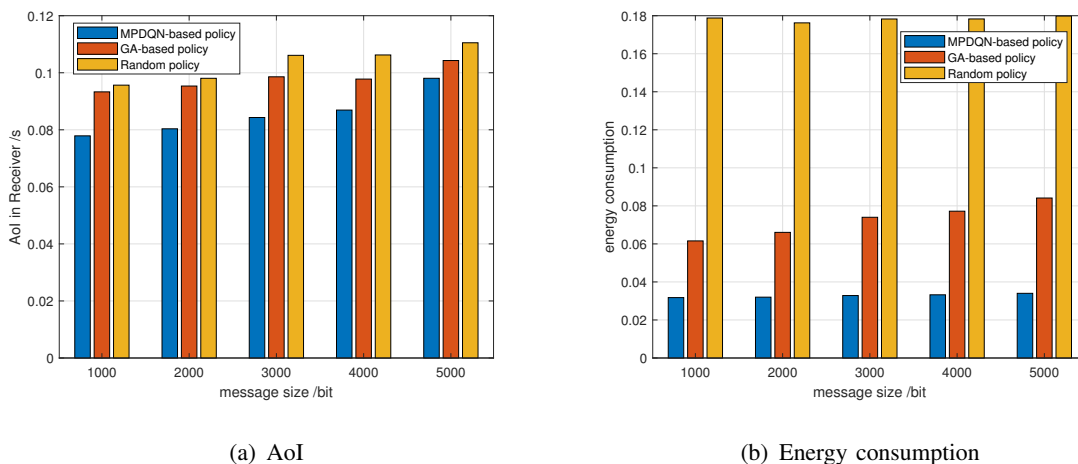(a) AoI   (b) Energy consumption

Fig. 10: The simulation results of each scheme for different packet size.

Fig. 10(a) compares the average AoI under different message sizes for MPDQN, GA algorithm, and random algorithm when the number of vehicles is 50. It can be observed that the average AoI at the receiver rises with the message size. This is because larger data packets not only increase the transmission delay at a constant power but also may lead to transmission failure when the transmission delay exceeds the time slots of the communication resources. However, both MPDQN and GA algorithms can mitigate this impact to some extent. Moreover, due to the real-time adjustment of RRI and power based on vehicle status, MPDQN achieves the best optimization effect on the average AoI at the receiver.

Fig. 10(b) compares the system average energy consumption under different message sizes for MPDQN, GA algorithm, and random algorithm when the number of vehicles is 50. It can be observed that under the random algorithm, there is almost no difference in average energy consumption. This is because when messages become larger, vehicles only transmit within a short time frame of the reserved resources, resulting in minimal impact on the energy consumption per transmission. This also explains why there is little difference in energy consumption under different message sizes for the other two algorithms. However, due to the impact on AoI, energy consumption under the other two algorithms increases to ensure lower AoI. On the other hand, under different message sizes, the average aggregate energy consumption of MPDQN is always lower than that of the random algorithm and GA algorithm. This is because MPDQN can adaptively select RRI and power for vehicles based on their current status, and by determining the resource occupancy frequency through RRI, it minimizes the average energy consumption within the system.

VI. Conclusions

This paper mainly focuses on the C-V2X vehicular network system, multiple message types, NOMA, DRL, and communication resource allocation issues to optimize the average AoI and transmission energy consumption. Firstly, for the case of multiple signal types in C-V2X, a multi-priority queue is adopted to reduce the AoI of high-priority messages in the queue, and NOMA technology is introduced to reduce the impact of communication processes on the AoI. Secondly, in the C-V2X scenario, the MPDQN algorithm is used to process vehicle status information, determine the optimal resource allocation strategy, and select RRI and power for the vehicles to minimize the AoI and energy consumption of the entire system. Simulation results show that our method not only maintains the stability of vehicle communication but also ensures the

timeliness of critical information, and outperforms baseline algorithms in optimizing average AoI and energy consumption.

REFERENCES

[1] L. Liu, C. Chen, Q. Pei, S. Maharjan, and Y. Zhang, "Vehicular edge computing and networking: A survey," *Mobile networks and applications*, vol. 26, pp. 1145–1168, 2021.

[2] Q. Wu, W. Wang, P. Fan, Q. Fan, H. Zhu, and K. B. Letaief, "Cooperative edge caching based on elastic federated and multi-agent deep reinforcement learning in next-generation networks," *IEEE Transactions on Network and Service Management*, 2024.

[3] J. Fan, S.-t. Yin, Q. Wu, and F. Gao, "Study on refined deployment of wireless mesh sensor network," in *2010 6th International Conference on Wireless Communications Networking and Mobile Computing (WiCOM)*, 2010, pp. 1–5.

[4] Q. Wu and J. Zheng, "Performance modeling and analysis of the adhoc mac protocol for vanets," pp. 3646–3652, 2015.

[5] F. Jing, W. Qiong, H. JunFeng, and F. Jing, "Optimal deployment of wireless mesh sensor networks based on delaunay triangulations," vol. 1, pp. V1–370–V1–374, 2010.

[6] W. Zhuang, Q. Ye, F. Lyu, N. Cheng, and J. Ren, "Sdn/nfv-empowered future iov with enhanced communication, computing, and caching," *Proceedings of the IEEE*, vol. 108, no. 2, pp. 274–291, 2019.

[7] G. Luo, C. Shao, N. Cheng, H. Zhou, H. Zhang, Q. Yuan, and J. Li, "Edgecooper: Network-aware cooperative lidar perception for enhanced vehicular awareness," *IEEE Journal on Selected Areas in Communications*, 2023.

[8] Z. Cui, X. Xiao, W. Qiong, F. Pingyi, F. Qiang, Z. Huiling, and W. Jiangzhou, "Anti-byzantine attacks enabled vehicle selection for asynchronous federated learning in vehicular edge computing," *China Communications*, vol. 21, no. 8, pp. 1–17, 2024.

[9] W. Qiong, S. Shuai, W. Ziyang, F. Qiang, F. Pingyi, and Z. Cui, "Towards v2i age-aware fairness access: A dqn based intelligent vehicular node training and test method," *Chinese Journal of Electronics*, vol. 32, no. 6, pp. 1230–1244, 2023.

[10] K. Wang, F. R. Yu, L. Wang, J. Li, N. Zhao, Q. Guan, B. Li, and Q. Wu, "Interference alignment with adaptive power allocation in full-duplex-enabled small cell networks," *IEEE Transactions on Vehicular Technology*, vol. 68, no. 3, pp. 3010–3015, 2019.

[11] Q. Wu, S. Xia, P. Fan, Q. Fan, and Z. Li, "Velocity-adaptive v2i fair-access scheme based on ieee 802.11 dcf for platooning vehicles," *Sensors*, vol. 18, no. 12, 2018. [Online]. Available: https://www.mdpi.com/1424-8220/18/12/4198

[12] J. Shen, N. Cheng, X. Wang, F. Lyu, W. Xu, Z. Liu, K. Aldubaikhy, and X. Shen, "Ringsfl: An adaptive split federated learning towards taming client heterogeneity," *IEEE Transactions on Mobile Computing*, 2023.

[13] J. Zhang, P. Fan, and K. B. Letaief, "Network coding for efficient multicast routing in wireless ad-hoc networks," *IEEE Transactions on Communications*, vol. 56, no. 4, pp. 598–607, 2008.

[14] Q. Wu, W. Wang, P. Fan, Q. Fan, J. Wang, and K. B. Letaief, "Urllc-aware resource allocation for heterogeneous vehicular edge computing," *IEEE Transactions on Vehicular Technology*, vol. 73, no. 8, pp. 11 789–11 805, 2024.

[15] Q. Wu, W. Wang, P. Fan, Q. Fan, H. Zhu, and K. B. Letaief, "Cooperative edge caching based on elastic federated and multi-agent deep reinforcement learning in next-generation networks," *IEEE Transactions on Network and Service Management*, vol. 21, no. 4, pp. 4179–4196, 2024.

[16] Q. Wu, Y. Zhao, Q. Fan, P. Fan, J. Wang, and C. Zhang, "Mobility-aware cooperative caching in vehicular edge computing based on asynchronous federated and deep reinforcement learning," *IEEE Journal of Selected Topics in Signal Processing*, vol. 17, no. 1, pp. 66–81, 2023.

[17] R. Wang, Z. Kan, Y. Cui, D. Wu, and Y. Zhen, "Cooperative caching strategy with content request prediction in internet of vehicles," *IEEE Internet of Things Journal*, vol. 8, no. 11, pp. 8964–8975, 2021.

[18] Q. Wang, D. O. Wu, and P. Fan, "Delay-constrained optimal link scheduling in wireless sensor networks," *IEEE Transactions on Vehicular Technology*, vol. 59, no. 9, pp. 4564–4577, 2010.

[19] P. Fan, C. Feng, Y. Wang, and N. Ge, "Investigation of the time-offset-based qos support with optical burst switching in wdm networks," in *2002 IEEE International Conference on Communications. Conference Proceedings. ICC 2002 (Cat. No. 02CH37333)*, vol. 5. IEEE, 2002, pp. 2682–2686.

[20] Q. Wu, H. Liu, C. Zhang, Q. Fan, Z. Li, and K. Wang, "Trajectory protection schemes based on a gravity mobility model in iot," *Electronics*, vol. 8, no. 2, 2019. [Online]. Available: https://www.mdpi.com/2079-9292/8/2/148

[21] Y. Dai, D. Xu, S. Maharjan, G. Qiao, and Y. Zhang, "Artificial intelligence empowered edge computing and caching for internet of vehicles," *IEEE Wireless Communications*, vol. 26, no. 3, pp. 12–18, 2019.

[22] Q. Wu, S. Wang, H. Ge, P. Fan, Q. Fan, and K. B. Letaief, "Delay-sensitive task offloading in vehicular fog computing-assisted platoons," *IEEE Transactions on Network and Service Management*, vol. 21, no. 2, pp. 2012–2026, 2023.

[23] ——, "Delay-sensitive task offloading in vehicular fog computing-assisted platoons," *IEEE Transactions on Network and Service Management*, vol. 21, no. 2, pp. 2012–2026, 2024.

[24] Q. Wu, S. Nie, P. Fan, H. Liu, F. Qiang, and Z. Li, "A swarming approach to optimize the one-hop delay in smart driving inter-platoon communications," *Sensors*, vol. 18, no. 10, 2018. [Online]. Available: https://www.mdpi.com/1424-8220/18/10/3307

[25] C. M. Silva, B. M. Masini, G. Ferrari, I. Thibault *et al.*, "A survey on infrastructure-based vehicular networks," *Mobile Information Systems*, vol. 2017, 2017.

[26] Z. Shao, Q. Wu, P. Fan, N. Cheng, Q. Fan, and J. Wang, "Semantic-aware resource allocation based on deep reinforcement learning for 5g-v2x hetnets," *IEEE Communications Letters*, vol. 28, no. 10, pp. 2452–2456, 2024.

[27] R. Molina-Masegosa and J. Gozalvez, "Lte-v for sidelink 5g v2x vehicular communications: A new 5g technology for short-range vehicle-to-everything communications," *IEEE Vehicular Technology Magazine*, vol. 12, no. 4, pp. 30–39, 2017.

[28] X. Wang, Q. Wu, P. Fan, Q. Fan, H. Zhu, and J. Wang, "Vehicle selection for c-v2x mode 4-based federated edge learning systems," *IEEE Systems Journal*, 2024.

[29] Q. Wu and J. Zheng, "Performance modeling of the ieee 802.11p edca mechanism for vanet," pp. 57–63, 2014.

[30] A. Nabil, K. Kaur, C. Dietrich, and V. Marojevic, "Performance analysis of sensing-based semi-persistent scheduling in c-v2x networks," in *2018 IEEE 88th vehicular technology conference (VTC-Fall)*. IEEE, 2018, pp. 1–5.

[31] Q. Wu and J. Zheng, "Performance modeling of ieee 802.11 dcf based fair channel access for vehicular-to-roadside communication in a non-saturated state," pp. 2575–2580, 2014.

[32] A. Dayal, V. K. Shah, B. Choudhury, V. Marojevic, C. Dietrich, and J. H. Reed, "Adaptive semi-persistent scheduling for enhanced on-road safety in decentralized v2x networks," in *2021 IFIP Networking Conference (IFIP Networking)*. IEEE, 2021, pp. 1–9.

[33] M. Ji, Q. Wu, P. Fan, N. Cheng, W. Chen, J. Wang, and K. B. Letaief, "Graph neural networks and deep reinforcement learning based resource allocation for v2x communications," *IEEE Internet of Things Journal*, 2024.

[34] Q. Wu, X. Wang, Q. Fan, P. Fan, C. Zhang, and Z. Li, "High stable and accurate vehicle selection scheme based on federated edge learning in vehicular networks," *China Communications*, vol. 20, no. 3, pp. 1–17, 2023.

[35] R. Deng, Y. Zhang, H. Zhang, B. Di, H. Zhang, H. V. Poor, and L. Song, "Reconfigurable holographic surfaces for ultra-massive mimo in 6g: Practical design, optimization and implementation," *IEEE Journal on Selected Areas in Communications*, vol. 41, no. 8, pp. 2367–2379, 2023.

[36] S. Yue, S. Zeng, L. Liu, Y. C. Eldar, and B. Di, "Hybrid near-far field channel estimation for holographic mimo communications," *IEEE Transactions on Wireless Communications*, 2024.

[37] D. Long, Q. Wu, Q. Fan, P. Fan, Z. Li, and J. Fan, "A power allocation scheme for mimo-noma and d2d vehicular edge computing based on decentralized drl," *Sensors*, vol. 23, no. 7, 2023. [Online]. Available: https://www.mdpi.com/1424-8220/23/7/3449

[38] B. Di, L. Song, Y. Li, and G. Y. Li, "Non-orthogonal multiple access for high-reliable and low-latency v2x communications in 5g systems," *IEEE journal on selected areas in communications*, vol. 35, no. 10, pp. 2383–2397, 2017.

[39] Y. Zhang, K. Peng, Z. Chen, and J. Song, "Sic vs. jd: Uplink noma techniques for m2m random access," in *2017 IEEE International Conference on Communications (ICC)*. IEEE, 2017, pp. 1–6.

[40] F. Wu, F. Lyu, J. Ren, P. Yang, K. Qian, S. Gao, and Y. Zhang, "Characterizing internet card user portraits for efficient churn prediction model design," *IEEE Transactions on Mobile Computing*, vol. 23, no. 2, pp. 1735–1752, 2023.

[41] F. Wu, F. Lyu, H. Wu, J. Ren, Y. Zhang, and X. Shen, "Characterizing user association patterns for optimizing small-cell edge system performance," *IEEE Network*, vol. 37, no. 3, pp. 210–217, 2022.

[42] J. Zhang, P. Fan, and K. B. Letaief, "Network coding for efficient multicast routing in wireless ad-hoc networks," *IEEE Transactions on Communications*, vol. 56, no. 4, pp. 598–607, 2008.

[43] P. Fan, C. Feng, Y. Wang, and N. Ge, "Investigation of the time-offset-based qos support with optical burst switching in wdm networks," vol. 5, pp. 2682–2686 vol.5, 2002.

[44] W. Wang, N. Cheng, M. Li, T. Yang, C. Zhou, C. Li, and F. Chen, "Value matters: A novel value of information-based resource scheduling method for cavs," *IEEE Transactions on Vehicular Technology*, 2024.

[45] Q. Wu, W. Wang, P. Fan, Q. Fan, J. Wang, and K. B. Letaief, "Urllc-awared resource allocation for heterogeneous vehicular edge computing," *IEEE Transactions on Vehicular Technology*, 2024.

[46] N. Cheng, F. Lyu, W. Quan, C. Zhou, H. He, W. Shi, and X. Shen, "Space/aerial-assisted computing offloading for iot applications: A learning-based approach," *IEEE Journal on Selected Areas in Communications*, vol. 37, no. 5, pp. 1117–1129, 2019.

[47] Z. Shao, Q. Wu, P. Fan, N. Cheng, W. Chen, J. Wang, and K. B. Letaief, "Semantic-aware spectrum sharing in internet of vehicles based on deep reinforcement learning," *IEEE Internet of Things Journal*, pp. 1–1, 2024.

[48] Q. Wu, S. Xia, Q. Fan, and Z. Li, "Performance analysis of ieee 802.11p for continuous backoff freezing in iov," *Electronics*, vol. 8, no. 12, 2019. [Online]. Available: https://www.mdpi.com/2079-9292/8/12/1404

[49] S. Song, Z. Zhang, Q. Wu, P. Fan, and Q. Fan, "Joint optimization of age of information and energy consumption in nr-v2x system based on deep reinforcement learning," *Sensors*, vol. 24, no. 13, 2024. [Online]. Available: https://www.mdpi.com/1424-8220/24/13/4338

[50] S. Leng and A. Yener, "Age of information minimization for wireless ad hoc networks: A deep reinforcement learning approach," in *2019 IEEE Global Communications Conference (GLOBECOM)*. IEEE, 2019, pp. 1–6.

[51] R. Sun, N. Cheng, C. Li, F. Chen, and W. Chen, "Knowledge-driven deep learning paradigms for wireless network optimization in 6g," *IEEE Network*, 2024.

[52] C. Zhang, W. Zhang, Q. Wu, P. Fan, Q. Fan, J. Wang, and K. B. Letaief, "Distributed deep reinforcement learning based gradient quantization for federated learning enabled vehicle edge computing," *IEEE Internet of Things Journal*, 2024.

[53] K. Qi, Q. Wu, P. Fan, N. Cheng, Q. Fan, and J. Wang, "Reconfigurable intelligent surface assisted vec based on multi-agent reinforcement learning," *IEEE Communications Letters*, vol. 28, no. 10, pp. 2427–2431, 2024.

[54] S. Leng and A. Yener, "Age of information minimization for an energy harvesting cognitive radio," *IEEE Transactions on Cognitive Communications and Networking*, vol. 5, no. 2, pp. 427–439, 2019.

[55] K. Qi, Q. Wu, P. Fan, N. Cheng, W. Chen, J. Wang, and K. B. Letaief, "Deep-reinforcement-learning-based aoi-aware resource allocation for ris-aided iov networks," *arXiv preprint arXiv:2406.11245*, 2024.

[56] R. D. Yates, Y. Sun, D. R. Brown, S. K. Kaul, E. Modiano, and S. Ulukus, "Age of information: An introduction and survey," *IEEE Journal on Selected Areas in Communications*, vol. 39, no. 5, pp. 1183–1210, 2021.

[57] C. M. W. Basnayaka, D. N. K. Jayakody, T. D. P. Perera, and M. V. Ribeiro, "Age of information in an urllc-enabled decode-and-forward wireless communication system," in *2021 IEEE 93rd Vehicular Technology Conference (VTC2021-Spring)*. IEEE, 2021, pp. 1–6.

[58] X. Gu, Q. Wu, Q. Fan *et al.*, "Mobility-aware federated self-supervised learning in vehicular network," *Urban Lifeline*, vol. 2, p. 10, 2024.

[59] X. Gu, Q. Wu, P. Fan, Q. Fan, N. Cheng, W. Chen, and K. B. Letaief, "Drl-based resource allocation for motion blur resistant federated self-supervised learning in iov," *IEEE Internet of Things Journal*, 2024.

[60] J. Hu, K. Yang, G. Wen, and L. Hanzo, "Integrated data and energy communication network: A comprehensive survey," *IEEE Communications Surveys & Tutorials*, vol. 20, no. 4, pp. 3169–3219, 2018.

[61] K. Qi, Q. Wu, P. Fan, N. Cheng, W. Chen, and K. B. Letaief, "Reconfigurable intelligent surface aided vehicular edge computing: Joint phase-shift optimization and multi-user power allocation," *IEEE Internet of Things Journal*, 2024.

[62] F. Abbas, P. Fan, and Z. Khan, "A novel low-latency v2v resource allocation scheme based on cellular v2x communications," *IEEE Transactions on Intelligent Transportation Systems*, vol. 20, no. 6, pp. 2185–2197, 2018.

[63] W. Li, X. Ma, J. Wu, K. S. Trivedi, X.-L. Huang, and Q. Liu, "Analytical model and performance evaluation of long-term evolution for vehicle safety services," *IEEE Transactions on Vehicular Technology*, vol. 66, no. 3, pp. 1926–1939, 2016.

[64] R. Molina-Masegosa and J. Gozalvez, "System level evaluation of lte-v2v mode 4 communications and its distributed scheduling," in *2017 IEEE 85th Vehicular Technology Conference (VTC Spring)*. IEEE, 2017, pp. 1–5.

[65] Y. Xu, Z. Qin, G. Gui, H. Gacanin, H. Sari, and F. Adachi, "Energy efficiency maximization in noma enabled backscatter communications with qos guarantee," *IEEE Wireless Communications Letters*, vol. 10, no. 2, pp. 353–357, 2020.

[66] H. Zhang, H. Zhang, W. Liu, K. Long, J. Dong, and V. C. Leung, "Energy efficient user clustering, hybrid precoding and power optimization in terahertz mimo-noma systems," *IEEE Journal on selected areas in communications*, vol. 38, no. 9, pp. 2074–2085, 2020.

[67] J.-B. Seo, B. C. Jung, and H. Jin, "Nonorthogonal random access for 5g mobile communication systems," *IEEE Transactions on Vehicular Technology*, vol. 67, no. 8, pp. 7867–7871, 2018.

[68] D. Ron and J.-R. Lee, "Drl-based sum-rate maximization in d2d communication underlaid uplink cellular networks," *IEEE Transactions on Vehicular Technology*, vol. 70, no. 10, pp. 11 121–11 126, 2021.

[69] D. Wang, H. Qin, B. Song, K. Xu, X. Du, and M. Guizani, "Joint resource allocation and power control for d2d communication with deep reinforcement learning in mcc," *Physical Communication*, vol. 45, p. 101262, 2021.

[70] B. S. Ciftler, A. Alwarafy, and M. Abdallah, "Distributed drl-based downlink power allocation for hybrid rf/vlc networks," *IEEE Photonics Journal*, vol. 14, no. 3, pp. 1–10, 2021.

[71] R. D. Yates and S. Kaul, "Real-time status updating: Multiple sources," in *2012 IEEE International Symposium on Information Theory Proceedings*. IEEE, 2012, pp. 2666–2670.

[72] Q. He, D. Yuan, and A. Ephremides, "Optimal link scheduling for age minimization in wireless systems," *IEEE Transactions on Information Theory*, vol. 64, no. 7, pp. 5381–5394, 2017.

[73] G. P. W. NBA, J. Haapola, and T. Samarasinghe, "A discrete-time markov chain based comparison of the mac layer performance of c-v2x mode 4 and ieee 802.11 p," *IEEE Transactions on Communications*, vol. 69, no. 4, pp. 2505–2517, 2020.

[74] Song, Shulin and Zhang, Zheng and Wu, Qiong and Fan, Pingyi and Fan, Qiang, "Joint optimization of age of information and energy consumption in NR-V2X system based on deep reinforcement learning," *Sensors*, vol. 24, no. 13, p. 4338, 2024.

[75] X. Zhang, S. Jin, C. Wang, X. Zhu, and M. Tomizuka, "Learning insertion primitives with discrete-continuous hybrid action space for robotic assembly tasks," in *2022 International Conference on Robotics and Automation (ICRA)*, 2022, pp. 9881–9887.

[76] H. Luo, Y. Bie, and S. Jin, "Reinforcement learning for traffic signal control in hybrid action space," *IEEE Transactions on Intelligent Transportation Systems*, pp. 1–17, 2024.

[77] G. Cecchini, A. Bazzi, B. M. Masini, and A. Zanella, "Ltev2vsim: An lte-v2v simulator for the investigation of resource allocation for cooperative awareness," in *2017 5th IEEE International Conference on Models and Technologies for Intelligent Transportation Systems (MT-ITS)*. IEEE, 2017, pp. 80–85.